

# The ALICE experiment

“ To see a World in a Grain of Sand  
And a Heaven in a Wild Flower  
Hold Infinity in the palm of your hand  
And Eternity in an hour ”

— William Blake  
(Auguries of Innocence)

The Large Hadron Collider (LHC) is the biggest and more powerful particle collider in the world. It consists of a 27 km ring of superconducting magnets and accelerating structures able to provide proton-proton and Lead-Lead collisions at the highest energies ever reached in laboratory to which the formation of the Quark Gluon Plasma is expected. While most of the LHC uptime is dedicated to the proton–proton physics that led to the discovery of the Higgs Boson [1, 2] and of two charmed pentaquark states [3], a significant part of the physics programme at the LHC is dedicated to heavy-ion physics and the characterisation of the Quark Gluon Plasma.

## 1.1 The Large Hadron Collider

The Large Hadron Collider is the last element of the accelerator complex at CERN (Figure 1.1), a succession of machines that accelerate particles to increasingly higher energies. Each element in this chain boosts the energy of a beam of particles, before injecting it into the next machine. Protons and heavy ions are brought to their collision energies through different acceleration chains.

The protons injected in the LHC ring start their journey in the LINAC2, where ionized hydrogen atoms are accelerated up to 50 MeV. Then the beam is injected in the Proton Synchrotron Booster (PSB), which accelerates protons up to 1.4 GeV and provides the beam bunches to the Proton Synchrotron (PS). The Proton Synchrotron provides 25 GeV protons to the Super Proton Synchrotron (SPS), where they are accelerated up to 450 GeV before the injection in the LHC.

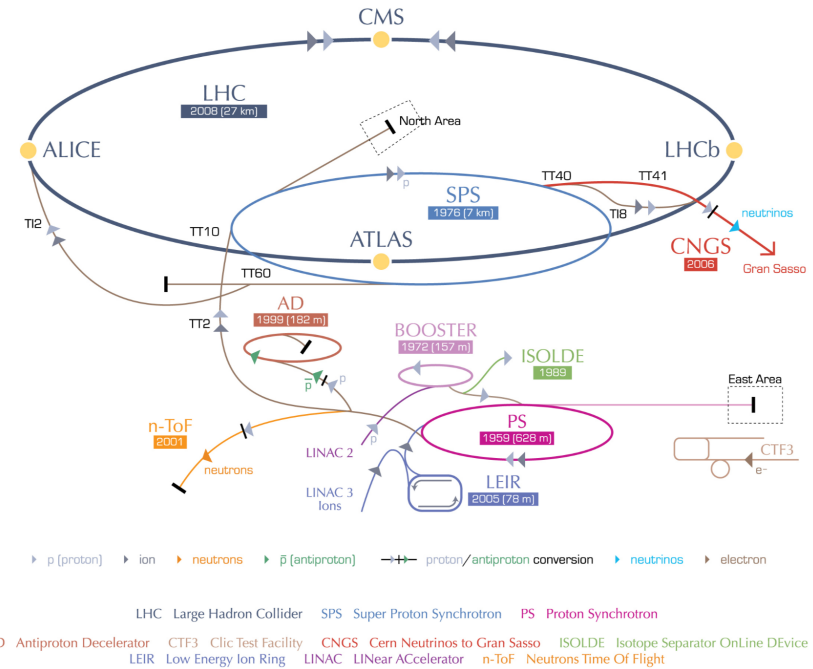


**Fig. 1.1:** Schematic view of the CERN accelerator complex and the LHC experiments [4].

Lead ions are produced from a highly isotopically pure  $^{208}\text{Pb}$  sample heated to a temperature of about  $800^\circ\text{C}$ . The lead vapour is ionized by an electron current. Many different charge states are produced with a maximum around  $\text{Pb}^{29+}$ . These ions are selected and accelerated to 4.2 MeV/u (energy per nucleon) before passing through a carbon foil, which strips most of them to  $\text{Pb}^{54+}$ . The  $\text{Pb}^{54+}$  beam is accumulated, then accelerated to 72 MeV/u in the Low Energy Ion Ring (LEIR), which transfers them to the PS. The PS accelerates the beam to 5.9 GeV/u and sends it to the SPS after first passing it through a second foil where it is fully stripped to  $\text{Pb}^{82+}$ . The SPS accelerates it to 177 GeV/u then sends it to the LHC, which accelerates it to 2.56 TeV/u.

The LHC ring is composed by 1232 dipole magnets and 392 quadrupole magnets, which respectively guide and focus the counter-rotating beams in separate vacuum-filled pipes. When the beams are stable they are brought into collision in four interaction points corresponding to the major LHC experiments. The top centre-of-mass energy reached at the LHC in the collisions are 13 TeV and 5.02 TeV per nucleon pair for pp and Pb–Pb collisions respectively.

Besides the centre-of-mass energy another crucial parameter for a collider is the luminosity delivered to the experiment. Indeed the number of events per second generated in the LHC collisions can be evaluated with the following formula:

$$R_{\text{event}} = L \sigma_{\text{event}} \quad (1.1)$$

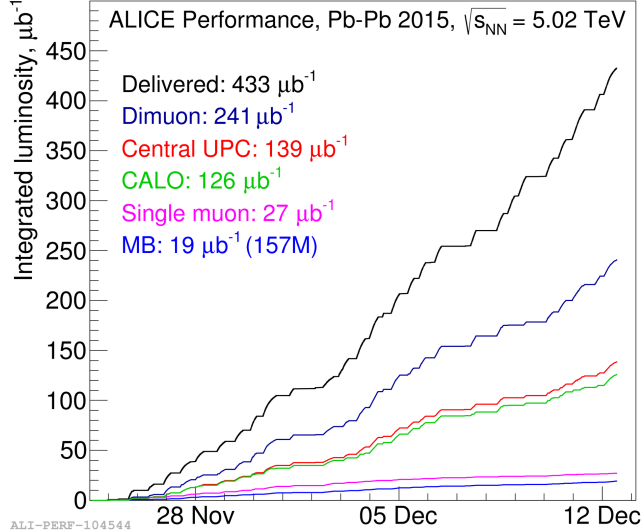


**Fig. 1.2:** ALICE delivered and integrated luminosity during the first Pb–Pb period in Run 2.

where  $L$  is the machine instantaneous luminosity and  $\sigma_{event}$  is the cross section for the event under study. The instantaneous luminosity depends only on the beam parameters and can be written as:

$$L = \frac{N_b N^2 f_{rev} \gamma}{4 \pi \epsilon_n \beta^*} F, \quad (1.2)$$

where  $N_b$  is the number of bunches in the collider ring,  $N$  is the number of charges in each bunch,  $f_{rev}$  is the revolution frequency of the beam,  $\gamma$  is the relativistic factor,  $\epsilon_n$  is the normalized emittance<sup>1</sup> and  $\beta^*$  is the value of the amplitude function<sup>2</sup> at the interaction point (IP) where the luminosity is estimated.

In order to maximise the luminosity of the LHC, the option of a p–p̄ collider was excluded due to the problem of the anti–protons production that is very complicated. The LHC can store up to 2808 bunches, with  $\sim 10^{11}$  protons per bunch, with 25 ns spacing [5]. The ALICE apparatus requires a peak luminosity of  $L = 10^{27} \text{ cm}^{-2}\text{s}^{-1}$  in Pb–Pb collisions. Figure 1.2 shows the delivered luminosity by the LHC (black line) and the integrated luminosities collected by ALICE, for different trigger configurations (colored lines), during the first Pb–Pb period in Run 2 at the end of 2015.

A crucial information for the collider experiments is the position where the collision between the two beams takes place: the *primary vertex*. The nominal position of the primary vertex is the origin of the coordinate reference frame of the experiment. Nevertheless, due to the finite size of the bunches the position of the

<sup>1</sup> $\epsilon_n = \beta \gamma \epsilon$  where  $\beta$  and  $\gamma$  are the usual relativistic factors and the emittance  $\epsilon$  is the spread of beam particles in the position-momentum phase space.

<sup>2</sup>The amplitude function  $\beta(s)$  describes the beam amplitude modulation due to the changing focusing strength.

primary vertex fluctuates around the nominal position. Being  $\sigma_{x,y,z}^{bunch}$  the *rms* of the bunch in the transverse and longitudinal direction, it can be shown that, assuming a gaussian profile of the bunches in the three directions, the *rms* of the vertex variation is:

$$\sigma_{x,y,z}^{vertex} = \frac{\sigma_{x,y,z}^{bunch}}{\sqrt{2}}, \quad (1.3)$$

where the *rms* size depends on the beam emittance and the amplitude function  $\beta^*$ :

$$\sigma_{x,y,z}^{bunch} = \sqrt{\frac{\epsilon_{x,y,z} \beta^*}{\sqrt{\pi}}}. \quad (1.4)$$

At the IP2, where the ALICE experiment is located, typical values for the vertex dispersion are  $\sigma_{x,y}^{vertex} \sim 50 \mu\text{m}$  and  $\sigma_z^{vertex} \sim 5 \text{ cm}$ .

## 1.2 ALICE design

The main goal of the ALICE experiment is the study of the QCD matter created in high energy heavy ion collisions, hence has been specifically designed and optimised [6, 7] for this purpose. An heavy ion experiment must have an efficient tracking system with a large acceptance and a good particle identification (PID) capabilities in a wide momentum range, especially at low momentum. Furthermore, it must work in an environment characterised by a large charged particle multiplicity. At the time of ALICE design, the charged particles multiplicity per rapidity unit in central Pb–Pb collisions was predicted to range between 2000 and 8000 [8], and for this reason detectors with high granularity and low material budget have been developed [6, 7].

The current layout of the ALICE experiment is shown in Figure 1.3 while Table 1.1 lists the position and the purpose of the ALICE sub-detectors. The ALICE coordinate system is a right-handed orthogonal Cartesian system with the origin settled at the nominal beams interaction point. The  $x$  axis is aligned with the horizontal accelerator plane and points to the centre of the LHC, the  $y$  axis is perpendicular to the accelerator plane and points upward. As a consequence the  $z$  axis is parallel to the beam direction and its positive direction is defined by the chirality of the coordinate system. For a more useful description of the apparatus and the physical quantities, two other coordinates are defined, which together with the  $z$  axis described above, form a cylindrical coordinate system: the azimuthal angle  $\phi$  increases counter-clockwise starting from  $\phi = 0$  for  $x$  axis looking towards the CMS side, and the polar

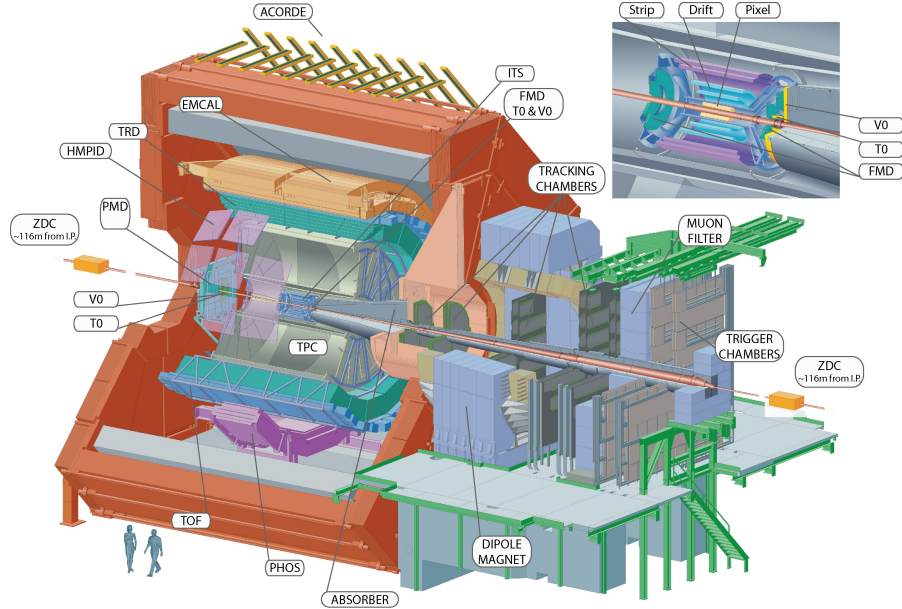


**Fig. 1.3:** The ALICE experimental setup and the red L3 solenoid magnet. The top right inset shows a zoom on the V0, T0, FMD and the ITS detectors.

angle  $\theta$  increases from  $z$  ( $\theta = 0$ ) to  $-z$  ( $\theta = \pi$ ). Another usefull variable, widely used in this thesis, is the *pseudo-rapidity*  $\eta$ :

$$\eta = \frac{1}{2} \ln \frac{|p| + p_z}{|p| - p_z} = -\ln \left[ \tan \left( \frac{\theta}{2} \right) \right]. \quad (1.5)$$

which, for ultra-relativistic objects, numerically converges to the *rapidity* already defined in the first chapter (Section ??).

In the ALICE apparatus, three main parts can be distinguished: the *central barrel*, the *muon spectrometer* and the *forward detectors*.

**Central Barrel** Consists of all the detectors located in the pseudo-rapidity range  $|\eta| < 0.9$ . The central barrel tracking detectors include the Inner Track- ing System (ITS), the Time Projection Chamber (TPC) and the Transition Radiation Detector (TRD), covering the full azimuthal acceptance. The central systems are dipped in a solenoidal magnetic field ( $B = 0.5$  T) produced by the warm resistive magnet previously used for the L3 experiment at LEP [10].

Detector	Acceptance			Main purpose
	Polar	Azimuthal	Position	
SPD <sup>†</sup> layer 1	$ \eta  < 2.0$	full	$r = 3.9 \text{ cm}$	tracking, vertex
SPD <sup>†</sup> layer 2	$ \eta  < 1.4$	full	$r = 7.6 \text{ cm}$	tracking, vertex
SDD layer 3	$ \eta  < 0.9$	full	$r = 15 \text{ cm}$	tracking, PID
SDD layer 4	$ \eta  < 0.9$	full	$r = 23.9 \text{ cm}$	tracking, PID
SSD layer 5	$ \eta  < 1.0$	full	$r = 38 \text{ cm}$	tracking, PID
SSD layer 6	$ \eta  < 1.0$	full	$r = 43 \text{ cm}$	tracking, PID
TPC	$ \eta  < 0.9$	full	$85 < r/\text{cm} < 247$	tracking, PID
TRD <sup>†</sup>	$ \eta  < 0.8$	full	$290 < r/\text{cm} < 368$	tracking, $e^\pm$ id
TOF <sup>†</sup>	$ \eta  < 0.9$	full	$370 < r/\text{cm} < 399$	PID
PHOS <sup>†</sup>	$ \eta  < 0.1$	$220^\circ < \phi < 320^\circ$	$460 < r/\text{cm} < 478$	photons
EMCal <sup>†</sup>	$ \eta  < 0.7$	$80^\circ < \phi < 187^\circ$	$460 < r/\text{cm} < 478$	photons, jets
HMPID	$ \eta  < 0.6$	$1^\circ < \phi < 59^\circ$	$r = 490 \text{ cm}$	PID
ACORDE <sup>†</sup>	$ \eta  < 1.3$	$30^\circ < \phi < 150^\circ$	$r = 850 \text{ cm}$	cosmics
PMD	$2.3 < \eta < 3.9$	full	$z = 367 \text{ cm}$	photons
FMD	$3.6 < \eta < 5.0$	full	$z = 320 \text{ cm}$	ch. particles
	$1.7 < \eta < 3.7$	full	$z = 80 \text{ cm}$	ch. particles
	$-3.4 < \eta < -1.7$	full	$z = -70 \text{ cm}$	ch. particles
V0 A <sup>†</sup>	$2.8 < \eta < 5.1$	full	$z = 329 \text{ cm}$	ch. particles
V0 C <sup>†</sup>	$-3.7 < \eta < -1.7$	full	$z = -88 \text{ cm}$	ch. particles
T0 A <sup>†</sup>	$4.6 < \eta < 4.9$	full	$z = 370 \text{ cm}$	time, vertex
T0 C <sup>†</sup>	$-3.3 < \eta < -3.0$	full	$z = -70 \text{ cm}$	time, vertex
ZDC <sup>†</sup>	$ \eta  > 8.8$	full	$z = \pm 113 \text{ cm}$	fwd neutrons
	$6.5 < \eta < 7.5$	$ \phi  < 10^\circ$	$z = \pm 113 \text{ cm}$	fwd protons
	$4.8 < \eta < 5.7$	$ 2\phi  < 32^\circ$	$z = \pm 113 \text{ cm}$	photons
MCH	$-4.0 < \eta < -2.5$	full	$-14.2 < z/\text{m} < -5.4$	muon tracking
MTR <sup>†</sup>	$-4.0 < \eta < -2.5$	full	$-17.1 < z/\text{m} < -16.1$	muon trigger

**Tab. 1.1:** Geometrical details and main purposes of the ALICE sub-detectors. This table has been taken and adapted from the description of the ALICE apparatus in [9]. The transverse ( $r$ ) and longitudinal ( $z$ ) coordinates as well as the acceptance (polar and azimuthal) are measured with respect to the ALICE coordinate reference frame, described in the text. When more than one position value is specified the detector is divided in two or several parts and the reported values are the minimum and maximum distances from the interaction point. The detectors marked with a dagger ( $\dagger$ ) are also used for triggering.

# Bibliography

1. ATLAS, Aad, G., *et al.* Observation of a new particle in the search for the Standard Model Higgs boson with the ATLAS detector at the LHC. *Physics Letters* **B716**, 1–29 (2012) (cit. on p. 1).
2. CMS, Chatrchyan, S., *et al.* Observation of a new boson at a mass of 125 GeV with the CMS experiment at the LHC. *Physics Letters* **B716**, 30–61 (2012) (cit. on p. 1).
3. LHCb, Aaij, R., Adeva, B., *et al.* Observation of  $J/\psi p$  Resonances Consistent with Pentaquark States in  $\Lambda_b^0 \rightarrow J/\psi K^- p$  Decays. *Physical Review Letters* **115**, 072001 (7 2015) (cit. on p. 1).
4. Lefèvre, C. *The CERN accelerator complex. Complexe des accélérateurs du CERN* 2008. <<https://cds.cern.ch/record/1260465>> (cit. on p. 2).
5. Evans, L. & Bryant, P. LHC Machine. *JINST* **3**, S08001 (2008) (cit. on p. 3).
6. ALICE, Carminati, F., Foka, P., *et al.* ALICE: Physics Performance Report, Volume I. *Journal of Physics G: Nuclear and Particle Physics* **30**, 1517 (2004) (cit. on p. 4).
7. ALICE, Fabjan, C. W., *et al.* ALICE: Physics performance report, volume II. *Journal of Physics G: Nuclear and Particle Physics* **G32** (eds Collaboration, A., Alessandro, B., Antinori, F., *et al.*) 1295–2040 (2006) (cit. on p. 4).
8. ALICE, Aamodt, K., *et al.* The ALICE experiment at the CERN LHC. *JINST* **3**, S08002 (2008) (cit. on p. 4).
9. ALICE, B., A., *et al.* Performance of the ALICE experiment at the CERN LHC. *International Journal of Modern Physics A* **29**, 1430044 (2014) (cit. on p. 6).
10. B., A. *et al.* The construction of the L3 experiment. *Nuclear Instruments and Methods in Physics Research A* **289**, 35–102 (1990) (cit. on p. 5).

